Online Supplemental material

Methods and Materials

Vertebrate Animals and reagents: All experiments conform to the protocols approved by the Institutional Animal Care and Use Committee. Eight-weeks-old Wild-type (WT) and IL-10 knockout (KO; $IL10^{tm1Cgn}$) male mice of C57BL/6J background were procured from Jackson Research Laboratory (Bar Harbor, ME). Male transgenic GFP-expressing (C57BL/6-Tg[CAGeGFP] 1Osb/J) mice served as a source of bone marrow-derived GFP^+ EPCs. The mice were allowed to acclimatize for 10 days under standard animal care conditions. Recombinant murine and human IL-10 and Stromal cell-derived factor 1α (SDF-1α) were obtained from R&D Systems (Minneapolis, MN). LPS and AMD3100 were obtained from Sigma Aldrich Inc (St. Louis, MO) and Curcurbitacin I and $CoCl_2$ from Calbiochem (San Diego, CA).

Bone marrow cell isolation and EPC culture: EPC isolation, *ex vivo* expansion and culture of EPCs was performed as previously described [1]. In brief, bone marrow mononuclear cells were isolated from mice by density-gradient centrifugation with Histopaque-1083 (Sigma) and macrophage-depleted by allowing attachment to uncoated plate for 1 hour. The unattached cells were removed and plated on culture dishes coated with 5μg/ml human fibronectin (Sigma) and cultured in phenol red–free endothelial cell basal medium-2 (EBM-2, Clonetics) supplemented with 5% FBS, vascular endothelial growth factor (VEGF)-A, fibroblast growth factor-2, epidermal growth factor, insulin-like growth factor-1, ascorbic acid, and antibiotics. Cells were cultured at 37 °C with 5% CO_2 in a humidified atmosphere. After 4 days in culture, non-adherent cells were removed by washing with PBS, new medium was applied, and the culture was maintained through day 7. EPCs, recognized as attaching spindle-shaped cells were used for further analysis and treatment.

Myocardial infarction and study design: Mice were subjected to myocardial infarction (MI) by ligation of left anterior descending coronary artery (LAD) as described previously [2-5]. Immediately after LAD ligation, one set of mice received intramyocardial injection of $5x10^4$ GFP+ EPC in a total volume of 15 μL at 5 different sites (basal anterior, mid anterior, mid lateral, apical anterior, and apical lateral) in the periinfarct area. These mice received either subcutaneous mouse recombinant IL-10 (50μg/kg b.w. per day; R&D Systems; EPC+IL-10 group) or saline (EPC+saline group) on 0, 1, 2, 3, 5 and 7 days post-MI. IL-10 dose is based on previous published data [4]. One set of mice with MI was administered IL-10 or saline, but no EPC cells (MI+IL-10 and MI+saline groups, respectively). The mice in sham group underwent the same procedure except for the LAD ligation. Inflammatory response and retention/survival of transplanted EPC was assessed after 3 days; LV functional changes on 7, 14 and 28 days and structural remodeling at 28 days post-MI.

Echocardiography: Transthoracic two-dimensional M-mode echocardiogram was obtained using Vevo 770 (VisualSonics, Toronto, Canada) equipped with 30 MHz transducer. Echocardiographic studies were performed before (baseline) and at 7, 14 and 28 days post-MI on mice anesthetized with a mixture of 1.5% isoflurane and oxygen (1 L/min). M-mode tracings were used to measure LV wall thickness, end-systolic diameter (LVESD) and end-diastolic diameter (LVEDD). The mean value of 9 measurements was determined for each sample. Percent fractional shortening (%FS) was calculated as described [6].

Morphometric studies: The hearts were perfusion fixed with 10% buffered formalin. Hearts cut into 3 slices (apex, mid-LV and base) and paraffin embedded. The morphometric analysis including infarct size and wall thickness and percent fibrosis was performed on Masson's trichrome stained tissue sections using ImageJ software (NIH, version 1.30, http://rsb.info.nih.gov/ij/). Wall thickness was measured perpendicular to the infarcted wall at three separate regions and averaged. Fibrosis area and total LV area was measured to determine percent fibrosis.

Immunofluroscence staining for EPC retention and engraftment in myocardial tissue: Immunofluorescence staining for tissue sections were performed as described previously [7]. Tissue sections were permeabilized and stained with anti-CD68 (Serotec, Raleigh, NC) for inflammatory cell infiltration and anti-CD31 antibody (BD Biosciences, San Jose, CA) for capillary density followed by incubation with respective secondary antibodies. Nuclei were counter-stained with 4', 6-diamidino-2-phenylindole (DAPI, 1:5000, Sigma Aldrich, St Louis, MO), and sections were examined with a fluorescent microscope (Nikon ECLIPSE TE200). The number of GFP^+ EPC (green) and their engraftment into the capillaries (CD-31 positive) and the associated inflammatory cell infiltration (CD-68 positive) were assessed in 10 randomly selected high-power visual fields (HVF) in the border zone of infarcted myocardium and expressed as number per HVF.

Terminal deoxynucleotidyl transferase–mediated dUTP nick end-labeling (TUNEL) staining for EPC survival in the myocardium: At 3d post-MI, survival of EPC in myocardium was determined by TUNEL staining on 4 μm thick paraffin-embedded sections as per manufacturer's instructions (Cell death detection assay, Roche, Indianapolis, IN). EPC's were GFP^+. DAPI staining was used to count the total number of nuclei. Apoptosis of transplanted EPCs was assessed by counting the number of GFP+/TUNEL+ cells per HVF.

Flow cytometry analysis (Fluorescence-activated cell sorting, FACS) to assess MI-induced EPC mobilization: While the above studies will clarify the effect of IL-10 on transplanted EPC survival and EPC-mediated myocardial repair, the studies will not establish the effect of IL-10 on bone marrow EPC mobilization and homing to injured myocardium. To investigate whether IL-10 affects MI-induced mobilization of BM-EPCs into the circulation, we performed myocardial infarction (MI) in wild-type (WT) and IL-10-knockout (KO) mice and assessed EPC mobilization (Sca-1+Flk1+ cells) by FACS analysis on peripheral blood mononuclear cells [8, 9] at 3 days post-MI. Freshly isolated mononuclear cells from peripheral blood (tail vein) by histopaque-1083 were stained with FITC-conjugated anti-mouse stem cell antigen 1 (Sca-1) and Phycoerythrin (PE)-conjugated anti-mouse fetal-liver kinase 1 (Flk1) antibodies and/or PE-conjugated CD31 antibodies (BD Pharmingen Inc.) in 0.1% PBS/BSA. Isotype-matched IgG antibodies were used as negative controls. Quantitative fluorescence analyses were performed with a LSR II flow cytometer (Becton Dickinson) and Flow-Jo Software (Tree Star, Inc.); 50,000 events were counted per sample. All groups were studied at least in triplicate.

Bone marrow transplantation (BMT) studies: We utilized BMT model to determine the effect of transplantation of bone marrow in IL-10 KO-mice with WT-marrow on EPC mobilization. Briefly, recipient IL-10-knockout (KO) mice were lethally irradiated with 9.0 Gy dose followed by BMT from donor wild-type (WT) mice (intravenous injection of $2X10^6$ donor BM cells). At 6 weeks after BMT (at which time bone marrow is reconstituted), recipient mice were subjected to MI surgery, as described in our

previous publications [2-5]. At day 3, MI-induced mobilization of EPCs was determined by FACS analysis on peripheral blood mononuclear cells.

***In vivo* SDF-1-induced EPC mobilization:** To determine if the IL-10 phenotype in IL-10 KO-mice was rescued by SDF-1 administration, a subset of mice that underwent MI surgery were immediately injected with mouse recombinant SDF-1α (500ng/mouse/day for three days; R & D Systems, Minneapolis, MN) via i.p injection and FACS analyses were performed for EPC mobilization at 3 days post-MI.

LPS or $CoCl_2$-mediated hypoxia-induced apoptosis or CXCR4 protein expression in EPC (*in vitro* studies): EPCs derived from bone marrow of WT (WT-EPC) and IL-10 KO mice (IL-10-deficient; KO-EPC) were grown on 8-well glass slides coated with 5 μg/ml human fibronectin (Sigma) and incubated with 100μM $CoCl_2$ for 24h [2, 4]. Apoptosis was assessed using TUNEL staining [2, 4] as per manufacturers instructions. Immunofluorecence staining for CXCR4 expression in EPCs were carried out using 1:100 anti-mouse CXC-chemokine receptor 4 (CXCR4) antibodies (Abcam, Cambridge, MA) and appropriate secondary antibody as described previously [7]. Nuclei were counter-stained with 4',6-diamidino-2-phenylindole (DAPI, 1:5000, Sigma Aldrich, St Louis, MO) and examined with a fluorescent microscope (Nikon ECLIPSE TE200). The index of apoptosis was calculated as the percentage of apoptotic myocyte nuclei/total number of nuclei (DAPI). Fluorescence intensity for CXCR4 signal (percent arbitrary fluorescence units, % AFU) was measured on 300 cells using ImageJ software. Results are presented as s.e.m. for three independent experiments.

Migration assay
The migration of EPCs (from WT and IL-10-deficient mice) toward a gradient of SDF-1 was performed in a 24-well Transwell Chamber (8.0 μm pore size, polycarbonate membrane, Corning Costar, Corning Incorporated Life Sciences, Acton, MA) as described earlier [1]. Briefly, 20 ng/mL SDF-1 (R&D Systems, Minneapolis, MN) in 600 μL of chemotaxis buffer (serum-free EBM-2, 0.1% BSA) was added to the lower compartment. EPCs (1×10^5 cells) in 100 μL of chemotaxis buffer were added to the upper compartment. Subsets of cells were incubated with CXCR4 inhibitor (AMD3100, 10μg/ml, Sigma-Aldrich Co.). After incubation at 37 °C for 18 h, the filters were removed and the cells that migrated through the pores of the membrane to the bottom chamber were stained with Hema-3® stain kit (Millipore, Billerica, MA) and counted manually in random high-power fields (~100) in each well. Data are expressed as number of cells that migrated through or invaded pores. All groups were studied at least in triplicate.

Quantitative RT-PCR: Tissue from border zone of the infarct was analyzed by quantitative real time PCR (RT-PCR) for mRNA expression of pro-inflammatory cytokines and chemokines (TNF-α, IL-1β, MCP-1 and IP-10) and SDF-1 as described previously [2, 4]. To assess VEGF expression in EPCs *in vitro*, EPCs were stimulated with IL-10 at a dose of 10 ng/ml for 4 hours and/or pretreated with curcurbitacin I (Cur I; stat3 inhibitor) at 1μM concentration for 30 minutes, unless otherwise indicated. Curcurbitacin I was used to determine if IL-10-induced VEGF expression was mediated through Stat3. RNA was collected from heart tissue or EPCs with RNA STAT-60 (TEL-TEST, Inc, Friendswood, Texas). Total RNA was reverse transcribed with iScript cDNA Synthesis Kit (Bio-Rad Laboratories, Hercules, CA), and amplification was performed using Taqman 7300 (Applied Biosystems, Foster City, CA). Relative mRNA expression of target genes was normalized to the endogenous 18s control gene (Applied Biosystems).

Statistical analyses: Data are presented as mean±SE. Between two groups of mice, an unpaired Student's *t*-test was performed to determine statistical significance. When involving more than two groups, ANOVA with Tukey posthoc test was used to analyze the data. Probability (P) values of <0.05 were considered a significant difference.

Supplemental Results

IL-10 enhances EPC-induced LV functional recovery after MI: Previous reports have suggested that EPC repairs injured myocardium by enhancing angiogenesis in the infarct myocardium. To determine if IL-10 promotes EPC repair capabilities, LV function was assessed by echocardiography as described earlier [4] at 7, 14 and 28 days, post-MI. LV end-systolic (LVESD) and -diastolic (LVEDD) dimensions were measured from m-mode tracing (Fig.7A) and percent ejection fraction (%EF) and fractional shortening (%FS) was calculated. Mice that received EPC showed improved function with reduced LVESD (#P<0.01 vs. MI, Fig.7B) and significantly increased %EF and %FS (#P<0.01 vs. MI, Fig.7C&D) at 28d, post-MI as compared to placebo (MI). Interestingly, IL-10 treatment robustly enhanced EPC-induced improvement in LV function with significant decrease in LVESD (*P<0.01 vs. EPC+saline, Fig.7B), and increase in %EF and %FS (*P<0.05 vs. EPC+saline; Fig.7C&D). LVEDD showed similar trends as LVESD (data not shown). Heart rates were not significantly different among the groups (data not shown).
Previous reports from our laboratories and by others have shown that EPC attenuates post-MI remodeling [7, 9-11]. To assess the influence of IL-10 on EPC-mediated effects on LV remodeling; infarct size and % fibrosis area was assessed as described previously [4] on Masson's trichrome stained heart sections using ImageJ software (NIH, version 1.30) at 28 days after MI. As expected, EPC significantly attenuated infarct size (34.13±0.65%, EPC+saline; 22.86±1.24%, EPC+IL10; Fig. 8A) and % fibrosis (#P<0.01 vs. MI; Fig.8B). Interestingly, IL-10 treated mice showed further reduction in infarct size and % fibrosis area (*P<0.01 vs. EPC+saline; Fig.8A&B).

Replacement of KO bone marrow by WT bone marrow attenuates MI-induced LV dysfunctions in IL-10 KO mice: We observed that a MI-induced EPC mobilization defect in KO-mice was attenuated by WT bone marrow transplantation (Fig. 1C). Our previous report has shown that LV function was significantly deteriorated in IL-10 KO-mice as compared to WT-mice at 28 days after MI [2]. We speculated that BMT in IL-10 KO-mice receiving WT bone marrow might improve MI-induced LV dysfunction. To address this, we performed BMT in IL-10 KO-mice (receiving WT-marrow; KO-BMT) and WT-mice (receiving IL-10-deficient marrow; WT-BMT). After 6 weeks, MI surgery was performed on these mice and LV function was assessed by echocardiography at 7, 14 and 28 days using m-mode tracings (Online Figure VII,A). Online Figure VII illustrates that KO-mice that received WT-marrow (KO-BMT) showed better LV function with reduced LVESD (P<0.05, Online Figure VII,B) and significantly increased %EF and %FS (P<0.05, Online Figure VII,C&D) as compared to WT-mice receiving IL-10 deficient bone marrow.

References

1. Yamaguchi J, Kusano KF, Masuo O, Kawamoto A, Silver M, Murasawa S, Bosch-Marce M, Masuda H, Losordo DW, Isner JM, Asahara T. Stromal cell-derived factor-1 effects on ex vivo expanded endothelial progenitor cell recruitment for ischemic neovascularization. *Circulation.* 2003;107(9):1322-1328.

2. Krishnamurthy P, Lambers E, Verma S, Thorne T, Qin G, Losordo DW, Kishore R. Myocardial knockdown of mRNA-stabilizing protein HuR attenuates post-MI inflammatory response and left ventricular dysfunction in IL-10-null mice. *Faseb J.* 2010.

3. Krishnamurthy P, Peterson JT, Subramanian V, Singh M, Singh K. Inhibition of matrix metalloproteinases improves left ventricular function in mice lacking osteopontin after myocardial infarction. *Mol Cell Biochem.* 2009;322(1-2):53-62.

4. Krishnamurthy P, Rajasingh J, Lambers E, Qin G, Losordo DW, Kishore R. IL-10 inhibits inflammation and attenuates left ventricular remodeling after myocardial infarction via activation of STAT3 and suppression of HuR. *Circ Res.* 2009;104(2):e9-18.

5. Krishnamurthy P, Subramanian V, Singh M, Singh K. Deficiency of beta1 integrins results in increased myocardial dysfunction after myocardial infarction. *Heart.* 2006;92(9):1309-1315.

6. Finsen AV, Christensen G, Sjaastad I. Echocardiographic parameters discriminating myocardial infarction with pulmonary congestion from myocardial infarction without congestion in the mouse. *J Appl Physiol.* 2005;98(2):680-689.

7. Ii M, Nishimura H, Iwakura A, Wecker A, Eaton E, Asahara T, Losordo DW. Endothelial progenitor cells are rapidly recruited to myocardium and mediate protective effect of ischemic preconditioning via "imported" nitric oxide synthase activity. *Circulation.* 2005;111(9):1114-1120.

8. Hamada H, Kim MK, Iwakura A, Ii M, Thorne T, Qin G, Asai J, Tsutsumi Y, Sekiguchi H, Silver M, Wecker A, Bord E, Zhu Y, Kishore R, Losordo DW. Estrogen receptors alpha and beta mediate contribution of bone marrow-derived endothelial progenitor cells to functional recovery after myocardial infarction. *Circulation.* 2006;114(21):2261-2270.

9. Iwakura A, Luedemann C, Shastry S, Hanley A, Kearney M, Aikawa R, Isner JM, Asahara T, Losordo DW. Estrogen-mediated, endothelial nitric oxide synthase-dependent mobilization of bone marrow-derived endothelial progenitor cells contributes to reendothelialization after arterial injury. *Circulation.* 2003;108(25):3115-3121.

10. Asahara T, Takahashi T, Masuda H, Kalka C, Chen D, Iwaguro H, Inai Y, Silver M, Isner JM. VEGF contributes to postnatal neovascularization by mobilizing bone marrow-derived endothelial progenitor cells. *Embo J.* 1999;18(14):3964-3972.

11. Asai J, Takenaka H, Kusano KF, Ii M, Luedemann C, Curry C, Eaton E, Iwakura A, Tsutsumi Y, Hamada H, Kishimoto S, Thorne T, Kishore R, Losordo DW. Topical sonic hedgehog gene therapy accelerates wound healing in diabetes by enhancing endothelial progenitor cell-mediated microvascular remodeling. *Circulation.* 2006;113(20):2413-2424.

Supplemental Figures

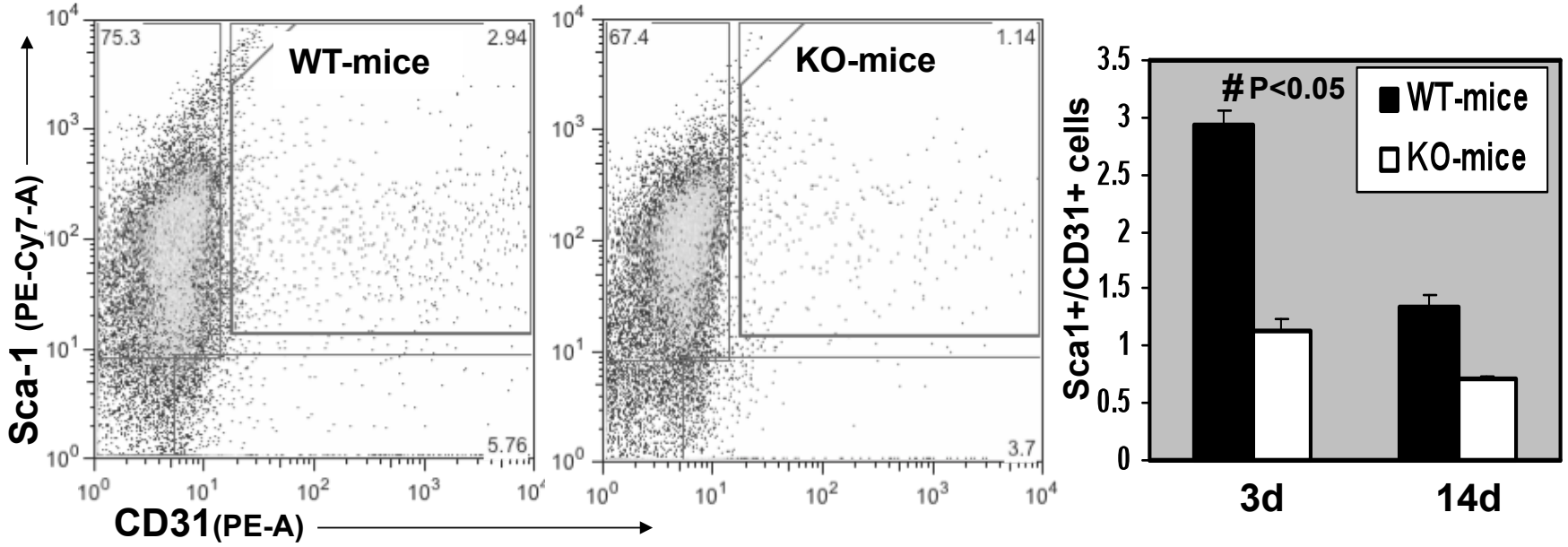

Online Figure I. FACS analysis on peripheral blood mononuclear cells for MI-induced Sca1+/CD31+ cells mobilization. Bar graph shows that Sca1+/CD31+ cells increased in WT-mice as compared to KO-mice at 3d post-MI (#p<0.05) and plateau at 14d post-MI.

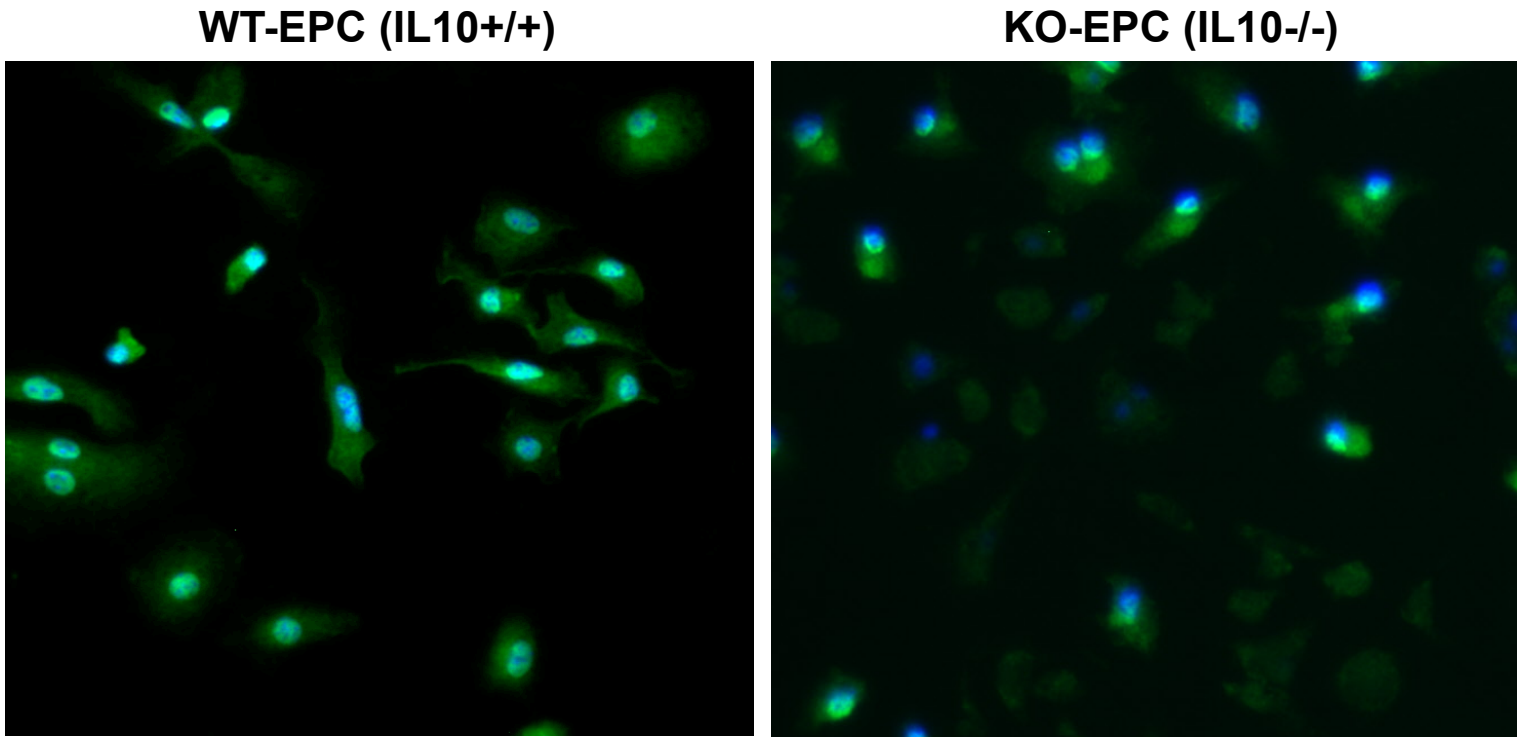

Online Figure II. Immunofluorescence staining for CXCR4 protein expression (green) [in response to CoCl2-induced hypoxia] in EPCs from WT (WT-EPC) and IL-10 KO-mice (KO-EPC) and DAPI (blue) for nuclear staining. Also, IL-10 deficient EPCs showed increased cell death (rounding and no clear nuclear staining).

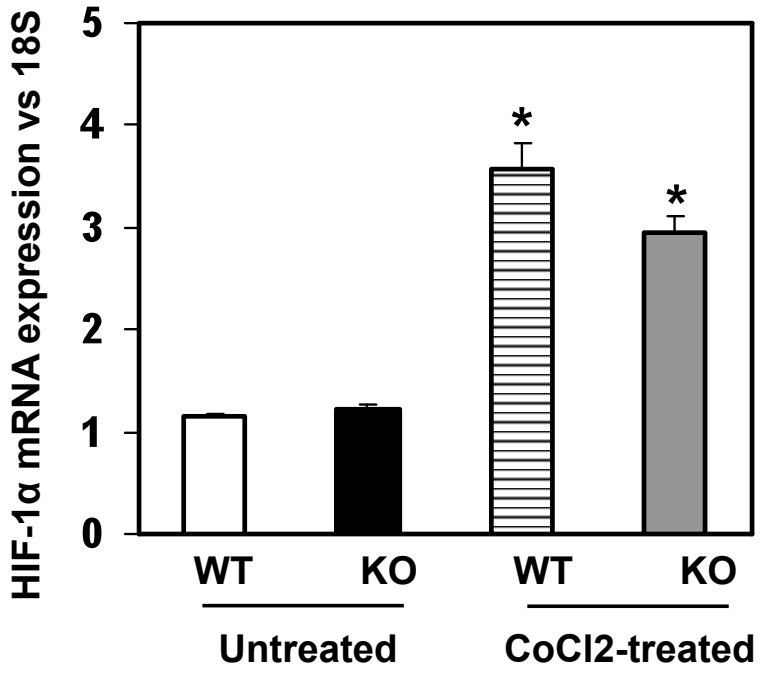

Online Figure III. Hypoxia (CoCl2)-induced HIF-1α mRNA expression in EPC's isolated from WT and IL-10 KO-mice. mRNA expression normalized to 18S expression. *P<0.01 vs untreated EPCs.

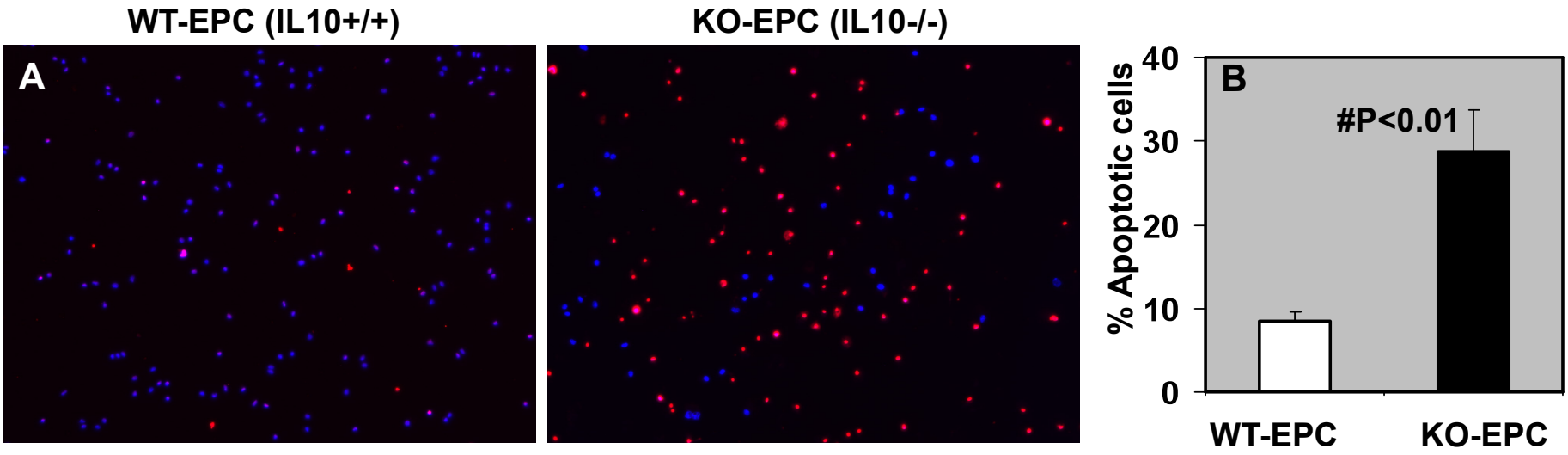

Online Figure IV. A. Hypoxia (CoCl2)-induced apoptosis (TUNEL+, red fluorescence) in EPC's isolated from WT and IL-10 KO-mice. DAPI (blue) was used for nuclear staining. **B.** CoCl2-induced EPC apoptosis was lower in WT-EPC as compared to EPC from KO-mice (#P<0.01).

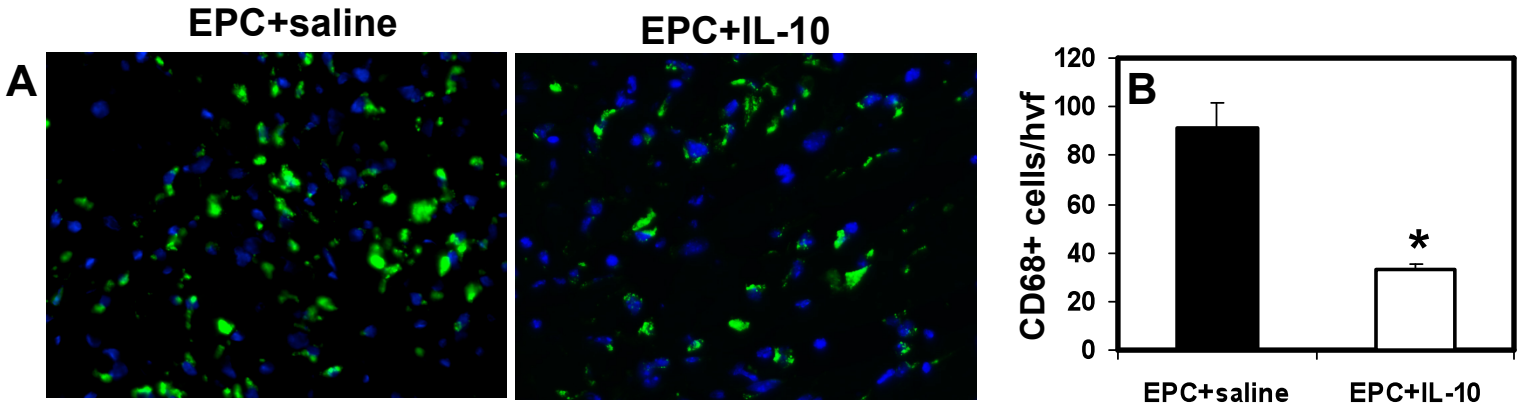

Online Figure V. A. Immunofluorescence staining for inflammatory cells (CD68-positive, green fluorescence) infiltration in the border zone of LV at 3 days post MI. **B.** Quantitative analysis of infiltrating CD68-positive cells at 3 days post-MI. IL-10 inhibited CD68+ cells infiltration as compared to MI and Sham hearts. *P<0.01 vs EPC+saline.

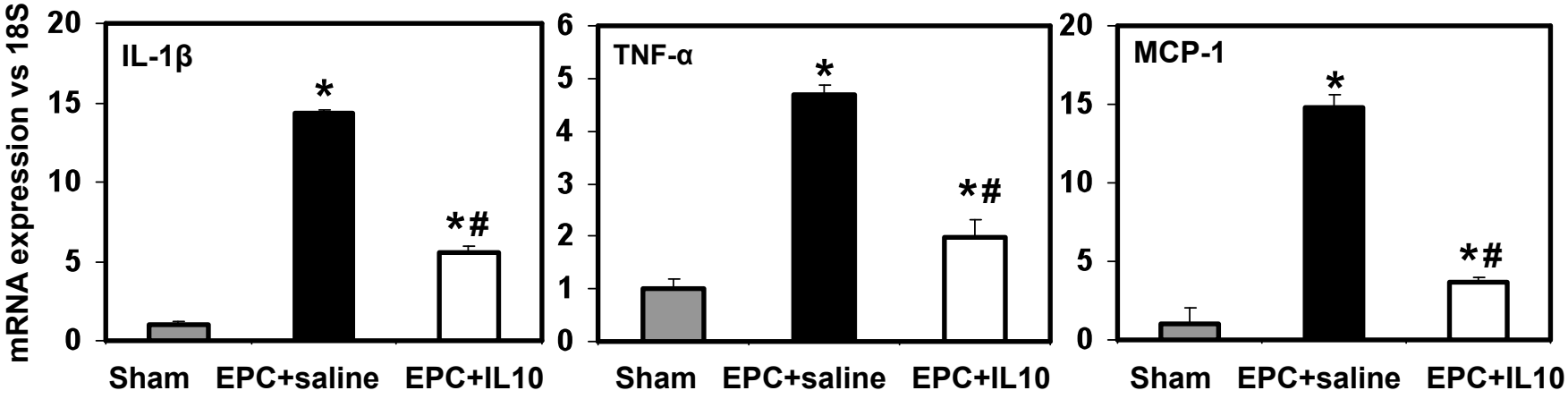

Online Figure VI. Quantitative analysis of mRNA expression of pro-inflammatory cytokines, chemokines in the border zone of LV infarct at 3 days post-MI. mRNA expression normalized to 18S expression and depicted as fold change vs Sham. *P<0.01 vs Sham; #P<0.05 vs EPC+saline.

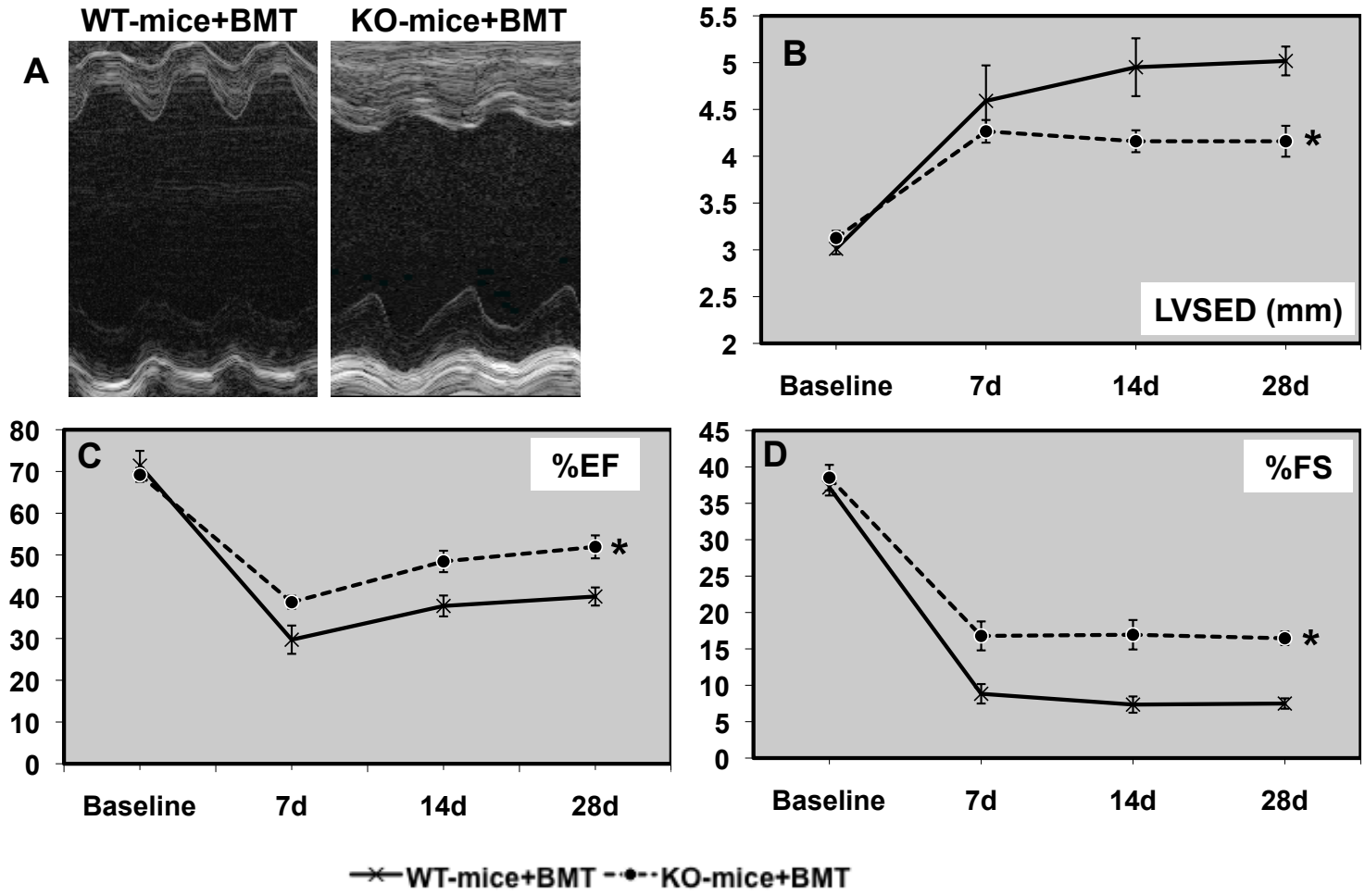

Online Figure VII. M-mode echocardiographic tracings at baseline and 7,14 and 28 days of MI in BM transplanted mice. Analysis of LV diameter in systole **(B)** and %EF **(C)** and %FS (**D)** calculations. WT-mice+BMT, WT-mice receiving IL-10 KO-marrow; KO-mice+BMT, KO-mice receiving WT-marrow. BMT in KO-mice showed improved LV function with decreased LVESD and increased %EF and %FS, as compared to WT-mice+BMT group. LVESD, LV end-systolic diameter; %EF, percent ejection fraction; %FS, percent fractional shortening; #P<0.05 vs MI; *P<0.05 vs WT-mice+BMT.